

# ICSV14

Cairns • Australia  
9-12 July, 2007



## **EXPERIMENTAL APPLICATION OF HIGH PRECISION K-SPACE FILTERS AND STOPPING RULES FOR FULLY AUTOMATED PNAH**

Rick Scholte, Ines Lopez, Bert Roozen, Henk Nijmeijer

Department of Mechanical Engineering  
Eindhoven University of Technology  
P.O. Box 513, 5600 MD Eindhoven, The Netherlands  
r.scholte@tue.nl

### **Abstract**

In general, inverse acoustic problems are ill-posed. Without any proper regularization action taken, noisy measurements result in an increasingly useless solution as the distance from the measurement plane to the desired source grows. Two distinctive steps take place in the regularization process for planar near-field acoustic holography (PNAH); first the low-pass filter function is defined and secondly a stopping rule is applied to determine the parameter settings of said filter. A number of well-known and newly developed filter functions and stopping rules are discussed and compared to one another, carefully listing the pros and cons. In acoustic imaging practice it has proven to be very hard to determine the right filter for a certain case combined with the automatic search for the near-optimal parameters. This paper presents a novel method that combines fitted filters for a broad number of possible experimental sources combined with highly efficient stopping rules, by taking advantage of k-space. Results based on actual measurements demonstrate the effectiveness, applicability and precision of the fully implemented and automated regularization process for PNAH. Implementations include modifications of Tikhonov, exponential and truncation low-pass filters, L-curve, Generalised Cross-Validation (GCV) and the novel Cut-Off and Slope (COS) parameter selection methods for PNAH.

### **1. INTRODUCTION**

Near-field Acoustic Holography dates back to the early 1980s when Williams [1] suggested that a large portion of source information is available in the near-field of a sound source. Evanescent waves attenuate with an exponential power as a function of distance from the sound source. To detect evanescent waves, a fine grid of measurement positions is required at a fixed distance from the source, yet within the near-field. The acquired field information is called a hologram, which contains all necessary information required to identify the sound source. Source information that is determined by calculation of the inverse solution of the wave equation. Noise in

the hologram measurements is very susceptible for blow-up in the inverse solution, especially at higher wavenumbers. A wide variety of methods to regularize ill-posed problems in general are discussed in [2], whereas more recently [3] focussed on regularization methods for NAH. This paper shortly discusses the basic PNAH theory, followed by a brief listing and discussion of regularization in k-space, which is split up in filter functions and stopping rules. More elaborate discussions, derivation and numerical analysis of said functions and methods can be found in [4]. Following the theoretical outline, the used measurement set-up and post-processing procedures are presented. The examined sources are two closely spaced holes in a large baffle connected to an isolated speaker at the back. The results of k-space application of five filter function combined with the two general stopping rules, GCV and L-curve, are illustrated. One of the main conclusions is the importance of a variable filter slope, combined with a stopping rule capable of handling two or more filter parameters. The COS iteration method with a modified exponential filter is such an example that demonstrates its effectiveness and accuracy in our automated PNAH measurement system.

## 2. PNAH AND REGULARIZATION THEORY

### 2.1. PNAH Discretization

The inverse solution to the acoustic wave equation by means of PNAH [5] for an infinitely wide plane to another infinitely wide plane in a continuous, source-free space for  $z > 0$  is exact. Due to practical limitations, namely the finite aperture and discrete spatial sampling, a discrete solution is required. A two-dimensional FFT determines the k-space spectrum from the discrete spatial measurements. The discrete solution of the wave-equation for a certain signal frequency  $f_s$  in k-space at the hologram distance  $z = z_h$  to a source distance  $z$  (for  $z > 0$ ) is a relatively straight-forward multiplication:

$$\hat{p}_d(k_x, k_y, z) = \hat{p}_d(k_x, k_y, z_h) e^{jk_z(z-z_h)}. \quad (1)$$

From 1 it follows that we need to determine  $k_z$  from the wavenumbers in both  $x$ - and  $y$ -direction, i.e.  $k_x$  and  $k_y$ , and the acoustic wavenumber  $k$  that follows from  $f_s$  and speed of sound  $c_0$ . In k-space  $k_z$  is determined by  $k_z = \pm \sqrt{k^2 - k_x^2 - k_y^2}$ , with  $k_{xy} = \sqrt{k_x^2 + k_y^2}$ . The radiation circle  $k_r$  is positioned at

$$k_{xy} = k = \frac{2\pi f}{c_0}. \quad (2)$$

For  $k_{xy} \leq k_r$  waves are propagating, whereas for  $k_{xy} > k_r$  waves are evanescent in nature. K-space provides a clear distinction of increasingly higher wavenumbers by moving outward from the center of the two-dimensional spectrum. Evanescent waves are most beneficial for providing spatially detailed information to the acoustic source image.

### 2.2. Low-Pass Filter Functions

The blow-up of noise at the source is generally suppressed by application of a low-pass k-space filter, cf. [4]. The resulting five filter functions are provided below, which are used in the regularization process of the experimental data. Firstly, the general form exponential filter

function is given by

$$H_f^{k_{co},\gamma} = \begin{cases} 1 - \frac{1}{2}e^{-(1-k_{xy}/k_{co})/\gamma}, & 0 < k_{xy} < k_{co}, \\ \frac{1}{2}e^{(1-k_{xy}/k_{co})/\gamma}, & k_{xy} \geq k_{co}, \end{cases} \quad (3)$$

where the slope is determined by the factor  $\gamma$  and the k-space cut-off  $k_{co}$ . The modified exponential filter, especially fit for near-field inverse problems, is given by

$$H_f^{k_{co},\phi} = \begin{cases} 1, & k_{xy} < k_{co} - k_{ev}\phi, \\ \frac{1}{2} + \frac{1}{2} \cos\left(k_{xy} - \frac{(k_{co}-k_{ev}\phi)}{2k_{ev}\phi}\pi\right), & k_{co} - k_{ev}\phi \leq k_{xy} \leq k_{co} + k_{ev}\phi, \\ 0, & k_{xy} > k_{co} + k_{ev}\phi, \end{cases} \quad (4)$$

where  $k_{ev}$  is the useful evanescent k-space content, or  $k_{ev} = k_{co} - k_r$ , and  $\phi$  the taper ratio between 0 and 1. Notice that this filter only affects information outside the radiation circle. The general form Tikhonov [6] filter function takes the inverse pressure to pressure propagation into account and is written as

$$H_f^\lambda(k_{xy}) = \frac{1}{1 + \lambda^2 e^{-2j\sqrt{k^2 - k_{co}^2}(z-z_h)}}, \text{ with } \lambda = e^{j\sqrt{k^2 - k_{co}^2}(z-z_h)}. \quad (5)$$

A high-pass filter function  $H_{f,hp}^\lambda(k_{xy})$  is used in a modification of the general form Tikhonov filter and adds a certain weight to the higher wavenumbers. This novel addition makes it possible to influence the filter slope behavior by inserting different high pass filters in the modified Tikhonov filter function:

$$H_f^\lambda(k_{xy}) = \frac{g_i^2}{g_i^2 + \lambda^2 (H_{f,hp}^\lambda(k_{xy}))^2}. \quad (6)$$

Any of the other low-pass filters can be written in their high-pass form and used in Equation (6). Finally, the low-pass truncation filter is simple and straight forward; it passes the band up to  $k_{co}$  and stops all wavenumbers higher than  $k_{co}$ :

$$H_f^{k_{co}} = \begin{cases} 1, & k_{xy} < k_{co}, \\ \frac{1}{2}, & k_{xy} = k_{co}, \\ 0, & k_{xy} > k_{co}. \end{cases} \quad (7)$$

### 2.3. Stopping Rules

For low-pass filter functions to become effective in inverse problems, their parameters need to be chosen carefully. Stopping rules provide an automated selection criterion based on a trade-off between perturbation and filter errors. In [4] three types of error estimate free stopping rules are derived for specific application in k-space. The first stopping rule is the L-curve criterium; a logarithmic plot of the perturbation versus the filter error. The vertical axis represents the norm of the inverse solution, which is bound to blow up while  $k_{co}$  increases (under-regularization),

and is written as

$$\eta(k_{co}) = \|\hat{p}_{sf}\|_2. \quad (8)$$

The horizontal axis exhibits the norm of the difference between the filtered and unfiltered data, thus indicating the error due to the filter:

$$\rho(k_{co}) = \|(\mathbf{H}_f - I_n)\hat{p}_h\|_2. \quad (9)$$

The point of maximum curvature between the horizontal and vertical part of the L-shaped curve is generally chosen as the near-optimal solution. The cut-off  $k_{co}$  that represents this point is used as the resulting filter cut-off. In discrete problems, an adaptive pruning algorithm is implemented to determine the point of maximum curvature [7].

The GCV [8] function in k-space has a global minimum value for  $k_{co}$ , which represents a trade-off between over-smoothing and blow-up of noise:

$$GCV(k_{co}) = \frac{\|(\mathbf{I} - \mathbf{H}_f^{k_{co}})\hat{p}_h\|_2}{Tr[(\mathbf{I} - \mathbf{H}_f^{k_{co}})\mathbf{G}]}, \quad (10)$$

where  $\mathbf{I}$  is the identity matrix and  $\mathbf{G}$  the forward propagation matrix. The numerator is dominated by the mean squared regularization error (comparable to the horizontal axis in the L-curve), while the denominator represents the perturbation error (vertical axis in the L-curve).

A newly developed method is the so-called COS iteration, which basically changes slope and cut-off of the modified exponential filter independently. The property that distinguishes this method is the importance of a variable filter slope and the significant influence on the results depending on the spatial properties of the measured field. Ordinary stopping criteria like GCV are used to determine the proper set. Practical difficulties in determining the point of maximum curvature in a three-dimensional L-curve, force the definition of a single minimizer as

$$\zeta(k_{co}, \phi) = \rho(k_{co}, \phi)\eta(k_{co}, \phi). \quad (11)$$

Cut-off  $k_{co}$  and slope  $\phi$  corresponding to the global minimum of  $\zeta$  are picked as modified exponential filter parameters, which is referred to as the  $\zeta$  criterium. For the practical cases both the GCV and  $\zeta$  criteria are applied for the COS iteration.

### 3. MEASUREMENT SET-UP AND POST-PROCESSING

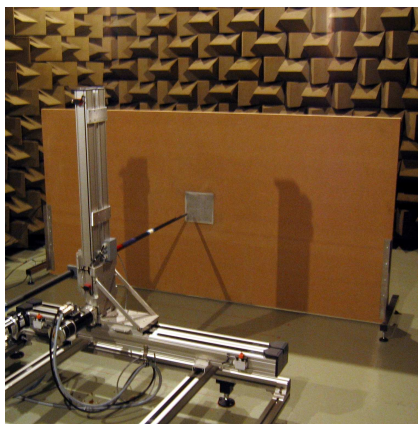
The measurement set-up used for the practical cases shown in the next section is situated in a semi-anechoic room (Figure 1). An automated traverse system (Figure 1c) moves a microphone beam (Figure 1a) over a pre-defined grid in front of the baffled source. The used sensor is a low-noise, omni-directional, miniature Sonion 8002 microphone with a typical diameter of only  $0.0025m$ . These small dimensions make the sensor very suitable for near-field measurements relatively close to a sound source, without disturbing the acoustic field due to its presence. Every grid measurement is carefully phase matched to the reference microphone at the back of the baffle, mounted in the tube that connects an isolated speaker to the back-plate of the aluminium baffle part, shown in Figure 1b. The tube is split up and connected to two channels in the center of the aluminium source plate, creating two coherent point sources with about  $0.04m$  horizontal



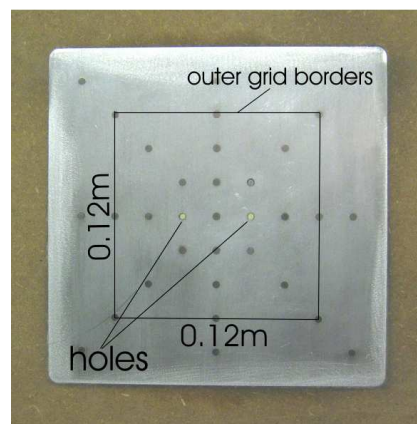
(a) microphone beam during measurement of a hologram position



(b) isolated speaker connected to the backside of the baffle



(c) overview of baffle and sensor traverse system in a semi-anechoic room



(d) close-up of the aluminium plate with various pattern possibilities

Figure 1. measurement setup of baffled point sources in a semi-anechoic room; the hologram is spatially sampled by a single miniature microphone mounted on a traversing beam

spacing between. The front-side view of these two sources is depicted in Figure 1d, the grid-size is  $25 \times 25$  points with  $0.005m$  spacing in horizontal and vertical direction.

The speaker inside the black box is excited by a Siglab data acquisition system connected to an amplifier, the measured pressures are fed back into the Siglab for post-processing. The control of the traverse system, excitation of the source, measurement and post-processing of all grid positions are fully integrated and automated by the in-house developed NAH software package. The post-processing software contains a regularization toolbox that incorporates all previously mentioned filters and stopping rules.

#### 4. EXPERIMENTAL RESULTS

The experimental results presented here are extracted from a large number of measurements as described in the previous section, at holograms with distances of  $z_h = 0.001m$  to  $z_h = 0.002m$  from the source. The influence of the filter functions and stopping rules is observed in Figure 2. The GCV generally manages to over-regularize compared to the L-curve criterium, which can be concluded from the differences in cut-offs that are found for the same filter function. Also, since the L-curve consistently manages to find a higher appropriate cut-off, the resulting source

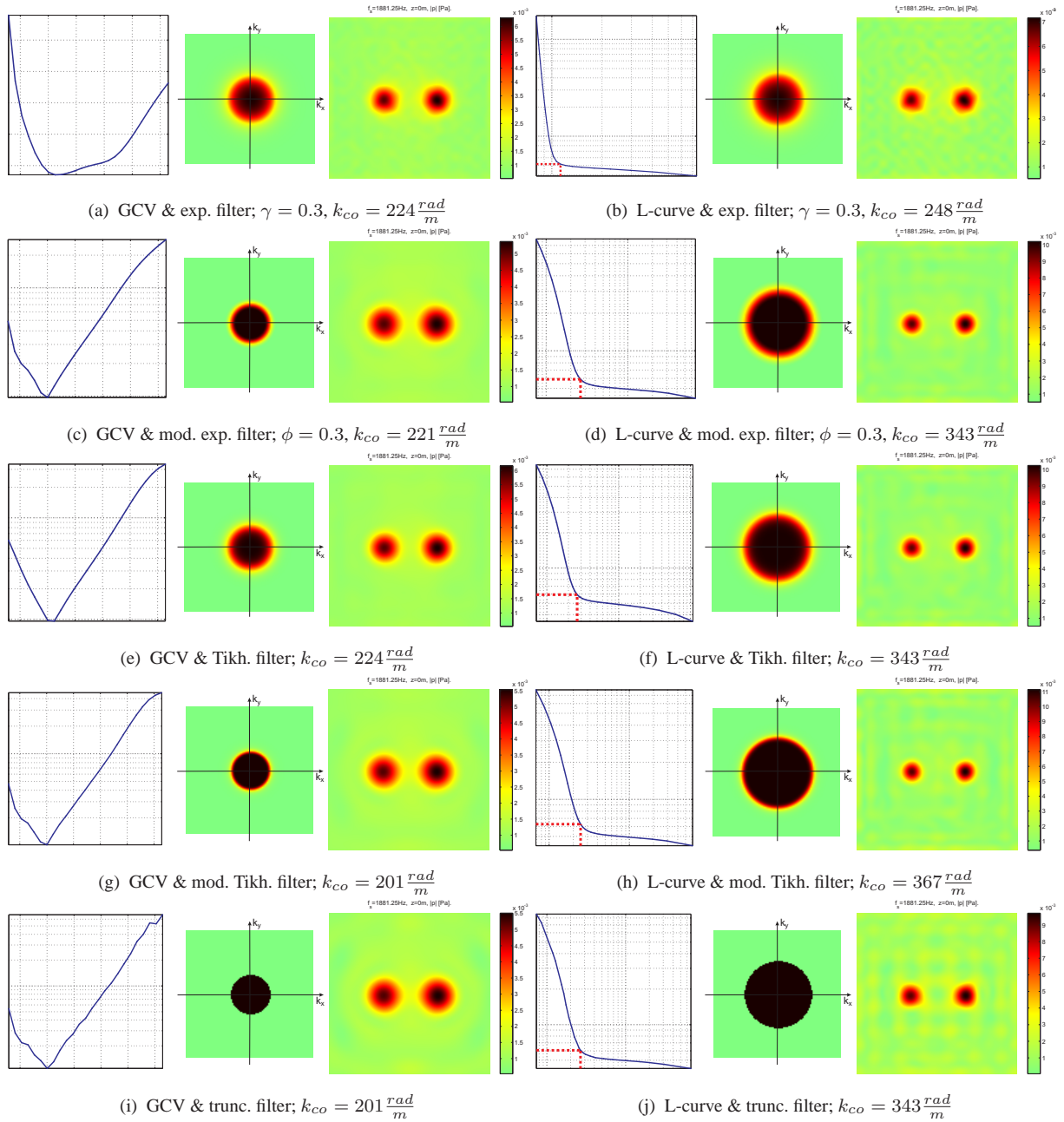
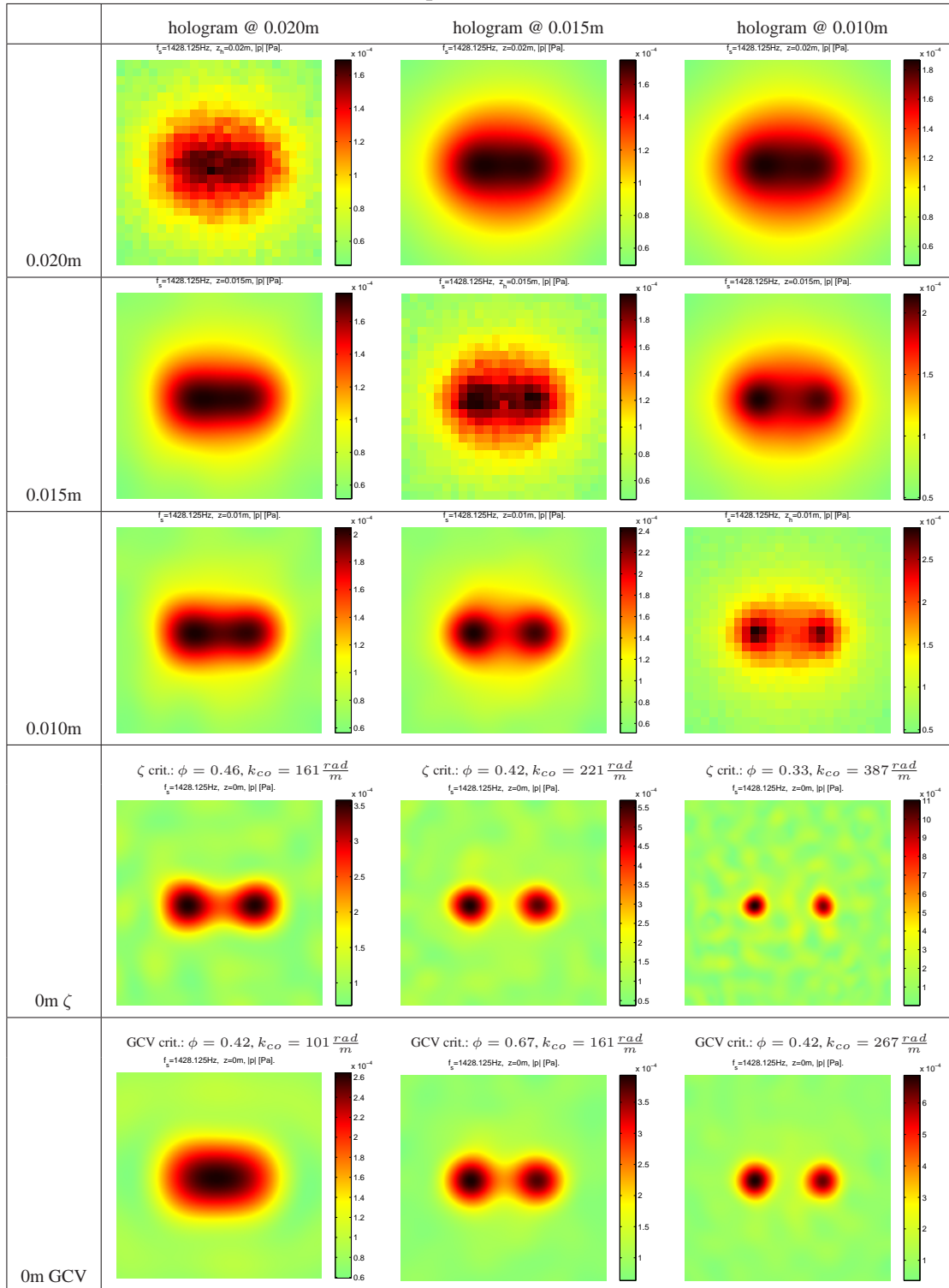


Figure 2. Comparison of five filter types combined with two stopping rules; leftmost plots show the stopping function (GCV or L-curve), center plots show the resulting low-pass filter and the rightmost plots provide the filtered result of PNAH at the source plane for  $f_s = 1881 Hz$  and  $z_h = 0.015 m$

images are sharper, of higher sound pressure level and closer to the spatial dimensions of the two point sources when compared to the GCV results. On the other hand, the L-curve results already show high influence of noise in the result, illustrating the trade-off between useful data and noise blow-up.

In all cases, the L-curve criterium creates clear L-shaped curves and the GCV functions show distinct global minima, thus regularization parameters are determined easily. Although most of the cut-offs of the respective stopping rules lie in the same range, the filter slopes differ considerably. The general form exponential and Tikhonov filters mainly show a very smooth slope, while the truncation filter ordinarily displays an infinitely steep slope. The modified exponential and Tikhonov filter slopes lie somewhere in between and are easily adjustable. Considering the

Table 1. Cut-Off and Slope iteration results at  $f_s = 1428Hz$ 


qualitative comparison, both Tikhonov filters and the modified exponential filter perform best when combined with the L-curve. The general form exponential filter's slope is too smooth to make a good trade-off between noise and high spatial changes thus showing a large portion of noise blow-up and too few spatially important source information. The truncation filter is the opposite; it allows high spatial changes, yet ringing artifacts due to the infinite slope tend to distort the results too much.

COS iteration with the GCV and  $\zeta$  criterium show clear differences in results at the source

plane, as can be observed from the images in Table 1. The results at  $0.02m$ ,  $0.015m$  and  $0.01m$  are either the measured holograms or results of  $\zeta$  COS filtered forward or backward PNAH solution. The  $\zeta$  criterium results with a hologram plane  $0.005m$  further away from the source than the hologram used as input for the GCV criterium based rule, show equal results at the source, meaning the  $\zeta$  criterium regularizes less and reveals more high spatial frequency information, without blowing up too much noise. Also the  $\zeta$  criterium solution at the source is by far the sharpest display of the actual point source size and displays the highest sound pressure levels, without blowing up noise. Not only does the  $\zeta$  criterium COS iteration perform well for this case, it has also shown to be the best choice for numerous other test cases that have been performed. Besides all the filter issues, this table illustrates the importance of hologram distance and the exponential loss of near-field information over very short distances.

## 5. DISCUSSION

The  $\zeta$  criterium based COS iteration combined with the modified exponential filter shows to be an automated regularization method that results in near-optimal solutions to the PNAH inverse process for a broad number of practical cases. This is due to the fact that the modified exponential filter is easily adjustable in both slope and cut-off, combined with an L-curve based criterium that is significantly more progressive compared to the GCV stopping rule. The GCV stopping rules mainly over-regularizes, which could in turn be the proper stopping rule when measurements contain low signal to noise ratios [4]. Five different filter functions for k-space application are given, combined with two stopping rules for filter parameter selection. A practical, qualitative comparison of these filters and stopping rules is given, resulting the sharpest source results for general and modified Tikhonov and modified exponential filters combined with the L-curve stopping rule. The presented results of the COS iteration are completely automatically generated, resulting in a fully automated and software implemented PNAH method.

### Acknowledgments

This research is supported by the Dutch Technology Foundation (STW).

### REFERENCES

- [1] E.G. Williams, “Holographic Imaging without the Wavelength Resolution Limit”, *Phys. Rev. Lett.* **45**, 554-557(1980).
- [2] P.C. Hansen, *Rank-Deficient and Discrete Ill-Posed Problems*, Technical University of Denmark, Lyngby, Denmark, 1996.
- [3] E.G. Williams, “Regularization methods for near-field acoustical holography”, *Journal of the Acoustical Society of America* **110**, 1976-1988(2001).
- [4] R. Scholte, “Wavenumber domain regularization for near-field acoustic holography by means of filter functions and stopping rules”, submitted (2007).
- [5] E. G. Williams, *Fourier Acoustics: Sound Radiation and Nearfield Acoustical Holography*, Academic, London, Great-Brittain, 1999.
- [6] A. N. Tikhonov, “Solution of incorrectly formulated problems and the regularization method”, *Soviet Math. Dokl.* **4**, 1035-1038(1963).
- [7] P.C. Hansen, “An adaptive pruning algorithm for the discrete L-curve criterion”, *J. Comp. Appl.* **198**, 483-492(2007).
- [8] P. Craven, “Smoothing Noisy Data with Spline Functions”, *Numer. Math.* **31**, 377-403(1979).